Arbitrary dispersion control of ultrashort optical pulses with acoustic waves

Frédéric Verluise, Vincent Laude, Jean-Pierre Huignard, and Pierre Tournois

Thomson-CSF, Corporate Research Laboratory, Domaine de Corbeville, F-91404 Orsay Cedex, France

Arnold Migus

Laboratoire pour l'Utilisation des Laser Intenses, Ecole polytechnique, Centre National de la Recherche Scientifique, Commissariat a l'Energie Atomique, Université Paris VI, Unité Mixte 7605, 91128 Palaiseau, France

Received March 1, 1999; revised manuscript received September 7, 1999

Acousto-optic programmable dispersive filters (AOPDF) can compensate in real time for large amounts of group-delay dispersion. This feature can be used in chirped-pulse amplification femtosecond laser chains to compensate adaptively for dispersion. An analytical expression relating the group delay at the output of the AOPDF to the input acoustic signal is obtained with coupled-wave theory in the case of collinear and quasi-collinear bulk acousto-optic interactions and also in the case of planar waveguides and optical fibers. With this relation, the acoustic signal that will induce an arbitrary group-delay variation with frequency can be easily obtained. Numerical simulations are shown to support the principle of arbitrary group-delay control with an AOPDF. © 2000 Optical Society of America [S0740-3224(00)01701-X]

OCIS codes: 230.1040, 320.1590, 320.5520, 320.5540.

1. INTRODUCTION

Even though femtosecond oscillators can deliver approximately dispersion-free laser pulses, the subsequent propagation through the amplifiers and the chirped-pulse amplification components introduces huge amounts of group-delay dispersion, which in turn broaden the pulse and generate artifacts. The importance of spectral phase control has been stressed by ultrafast laser users who typically need extremely short pulses but with no pedestals and with a given temporal shape. This calls for programmable devices capable of compensating for large amounts of dispersion over large spectral bandwidths. Most pulse-shaper devices that have been proposed are based on the use of liquid-crystal spatial light modulators in the Fourier plane of a zero-dispersion line (see, e.g., Refs. 1–6). The main drawbacks of such systems are a limited dynamic range and the coupling of the spatial and temporal aberrations of the laser beam.

Recently, the use of an integrated acousto-optic tunable filter for pulse shaping was proposed,[7] and the implementation of a notch filter was demonstrated in a bandwidth of ~8 nm around 1530 nm. However, in an integrated acousto-optic tunable filter, although the frequency of the acoustic wave is an adjustable constant, it does not allow for true control of the optical spectral phase. Tournois later proposed the use of a collinear acousto-optic interaction in a bulk device termed an acousto-optic programmable dispersive filter (AOPDF)[8] and in a first experiment demonstrated the compression of Ti:sapphire femtosecond pulses in the 100-fs range with a tellurium dioxide (TeO_2) acousto-optic modulator. In Tournois' design the acousto-optic interaction is collinear to maximize the interaction length, whereas the acoustic frequency is a variable function of time and provides control over the group delay of the diffracted optical pulse. Note that the acousto-optic modulator used experimentally by Tournois was not designed for collinear interaction but was still able to provide for the desired dispersion. The AOPDF in collinear configuration is in principle free of spatiotemporal coupling effects and can provide for large dispersion compensation ranges; it thus overcomes the two main limitations of spatial light modulator–based zero-dispersion lines. Deviations from this ideal behavior when a quasi-collinear interaction is used will be discussed in Subsection 4.B.

Our goals in this paper are to demonstrate that an arbitrary, although monotonic, variation of the group delay can be added to an optical short pulse with a frequency-modulated acoustic wave and to provide for expressions that relate the induced optical group delay to the acoustic instantaneous frequency. These expressions can be used either for predicting the dispersion characteristics of the optical pulse when it leaves the acousto-optic crystal or, more interestingly, for computing the acoustic wave function needed to control the optical group delay arbitrarily. This arbitrary control has immediate applications to adaptive dispersion compensation in chirped-pulsed amplification laser chains and to femtosecond pulse shaping.

The paper is organized as follows. In Section 2 we will present a simple phenomenological description of the principle used for arbitrary group-delay control. In Section 3 coupled-wave theory[9] will be used to model the interaction accurately and will be shown to support the previous phenomenological model. In Section 4 the practical issues arising when volume gratings in acousto-optic crystals are created will be considered, and numerical simulations will illustrate the operation of a quasi-collinear TeO_2 AOPDF.

2. PHENOMENOLOGICAL APPROACH

The idea underlying the control of the optical group delay with an acousto-optic interaction as proposed by Tournois[8] is depicted in Fig. 1. Suppose an acoustic wave is launched in an acousto-optic device by use of a transducer excited by a rf temporal signal as is usual in acousto-optics. The acousto-optic interaction can be either a bulk collinear or a quasi-collinear interaction, in which case the optical modes can be approximated by plane waves, or an acousto-optic interaction in a waveguide or optical fiber, in which case the transverse profile of the optical modes must be taken into account. The acoustic wave propagates with a certain velocity V along the z axis and hence reproduces spatially the temporal shape of the rf signal. As the velocity of optical waves is usually much larger than that of the acoustic wave, and because we assume ultrashort optical pulses in the picosecond or femtosecond range, the incident optical pulses will see a fixed dielectric grating inside the device. We neglect here and in the following the small Doppler frequency shift that is always present with acousto-optic interactions. Let us now assume that the rf signal is chirped; i.e., its instantaneous frequency is a continuously varying function of time. The acoustic wave will then reproduce this behavior spatially, and its local spatial frequency will also be chirped. It is well known[9] that two optical modes can be coupled efficiently by an acousto-optic interaction only in the case of phase matching between the two optical modes and the acoustic wave. Since locally there is only one spatial frequency in the acoustic grating, only one optical frequency can be diffracted at a certain position z. This situation is depicted in Fig. 1. The incident optical short pulse has a spectrum extending from ω_a to ω_b and is initially in mode 1. Every frequency ω between ω_a and ω_b travels a certain distance before it encounters a phase-matched spatial frequency in the acoustic grating. At this position $z(\omega)$, part of the energy in mode 1 is diffracted into mode 2 and travels subsequently on that mode. For simplicity, the polarizations of both modes are assumed orthogonal, but this requirement is not compulsory for the principle of the AOPDF. The pulse leaving the device on mode 2 will be made of all spectral components that have been diffracted at various positions. If the velocities of the two modes are different, then each frequency will see a different time delay. Then by properly choosing the temporal form of the rf signal, and hence the spatial form of the acoustic wave, we can create an almost arbitrary group-delay distribution as a function of frequency. This physical discussion qualitatively explains the principle of the AOPDF, but to obtain the exact relation between the optical group delay and the acoustic wave we propose to formalize it on the basis of coupled-wave theory in Section 3. However, the mathematics therein are a direct transcription of the physical analysis of this section.

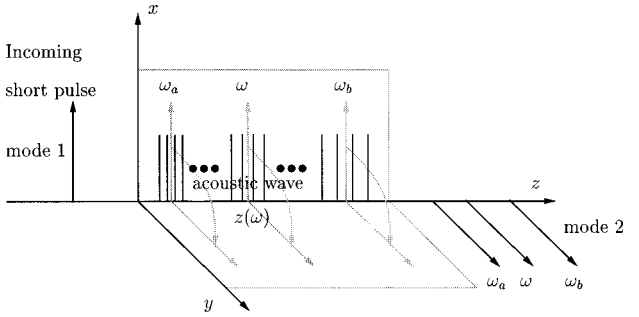

Fig. 1. Schematic representation of the AOPDF principle. The acoustic wave and the incident and diffracted optical waves are collinear and propagating along the z axis. See text for details.

3. COUPLED-WAVE ANALYSIS

A. Notations

We consider a fixed dielectric perturbation in a birefringent crystal that is directed along the z axis and is created by an acoustic wave. We use the approximation of the fixed dielectric perturbation, since the light velocity is much larger than the acoustic velocity as discussed in Section 2. We assume that the acoustic wave is a frequency-modulated signal, so that the dielectric perturbation reads as

$$\epsilon(z) = \epsilon + 2\epsilon_1(z)\cos[\psi(z)], \tag{1}$$

with the acoustic phase given by

$$\Psi(z) = \int_0^z K(z)\mathrm{d}z. \tag{2}$$

Here ϵ is the unperturbated dielectric tensor, which has only diagonal elements in the reference frame of Fig. 1, $\epsilon_1(z)$ is the perturbated part of the dielectric tensor that will result in coupling of the optical modes, and $K(z)$ is the instantaneous spatial frequency of the acoustic wave. To simplify the mathematical derivations, we will assume that $K(z)$ is a monotonic function of z; i.e., it is either increasing or decreasing. This assumption is not strictly required for the AOPDF principle to apply; however, it is needed to define the function $z(\omega)$ introduced physically in Section 2 and used extensively in this section. The possible amplitude variations of the acoustic wave are contained in $\epsilon_1(z)$, but they are not central to the present discussion and are indicated here only for completeness. Note that usually $\epsilon_1(z)$ is much smaller than ϵ, so that only its off-diagonal elements need to be considered.

The two optical modes are also propagating along the z axis in the direction of positive z; the case of quasi-collinear optical modes and the acoustic wave will be treated in Subsection 4.B. The optical pulses can be represented as a spectral superposition:

$$\mathbf{E}(t, \mathbf{r}) = \int \mathbf{E}(\omega, \mathbf{r})\exp(i\omega t)\mathrm{d}\omega. \tag{3}$$

In the following we implicitly consider separately the propagation of the different angular frequencies ω that make up the spectrum of the optical pulses. When no acoustic wave is applied, the modes are plane waves whose electric field vectors can be written as

$$\mathbf{E}_m(\omega, \mathbf{r}) = \sqrt{S(\omega)}\mathbf{e}_m \exp[-ik_m(\omega)z], \tag{4}$$

with $m = 1, 2$, $k_m(\omega) = n_m(\omega)\omega/c$, and where

$$\mathbf{e}_m = \left[\frac{2\mu_0\omega}{k_m(\omega)}\right]^{1/2} \mathbf{p}_m. \tag{5}$$

$\mathbf{p}_m$, $m = 1, 2$, are the unit vectors describing the polarization of the waves and are assumed to be along the ordinary and extraordinary axes, respectively, so that $n_1 = n_0$ and $n_2 = n_e$; furthermore, $\mathbf{p}_1 \cdot \mathbf{p}_2 = 0$. $\mathbf{e}_m$ is normalized so as to represent a power flow of 1 W/cm^2 in the z direction,[9] and $S(\omega)$ gives the proportion of this power flow for every frequency in the power spectrum of the pulse.

B. Wave-Equation Solution

The electric field vector in the crystal must satisfy the following wave equation:

$$\frac{\mathrm{d}^2}{\mathrm{d}z^2}\mathbf{E}(\omega, \mathbf{r}) + \omega^2\mu_0\epsilon(z)\mathbf{E}(\omega, \mathbf{r}) = 0. \tag{6}$$

This second-order differential equation depends only on z, and its solution is given by Eq. (4) in the case $\epsilon_1(z) = 0$. Its general solution can be written as

$$\mathbf{E}(\omega, \mathbf{r}) = \sqrt{S(\omega)}\{A_1(z)\mathbf{e}_1 \exp[-ik_1(\omega)z] + A_2(z)\mathbf{e}_2 \exp[-ik_2(\omega)z]\}, \tag{7}$$

where $A_m(z)$, $m = 1,2$ are arbitrary but supposedly slowly varying functions of z. By inserting Eqs. (1) and (7) into Eq. (6), neglecting the second derivative of $A_m(z)$, and projecting the resulting equation on $\mathbf{e}_1$ and $\mathbf{e}_2$, respectively, we are led to the following coupled-wave equations:

$$\frac{\mathrm{d}}{\mathrm{d}z}A_1(z) = -i\kappa(z)A_2(z)\{\exp[-i\phi_+(z)] + \exp[-i\phi_-(z)]\}, \tag{8}$$

$$\frac{\mathrm{d}}{\mathrm{d}z}A_2(z) = -i\kappa(z)A_1(z)\{\exp[i\phi_+(z)] + \exp[i\phi_-(z)]\}, \tag{9}$$

with

$$\phi_\pm(z) = [k_2(\omega) - k_1(\omega)]z \pm \psi(z), \tag{10}$$

$$\kappa(z) = \frac{\omega^2\mu_0}{2[k_1(\omega)k_2(\omega)]^{1/2}}\mathbf{p}_1 \cdot \epsilon_1(z) \cdot \mathbf{p}_2. \tag{11}$$

It is well known[9] that with coupled-wave equations like Eqs. (8) and (9), nonnegligible energy transfer between the two modes is obtained only in the case of phase matching between optical and acoustic waves, that is,

$$\frac{\mathrm{d}}{\mathrm{d}z}\phi_\pm(z) = 0 = k_2(\omega) - k_1(\omega) \pm K(z). \tag{12}$$

The choice of the sign in this equation depends solely on the sign of $k_2 - k_1$, i.e., on the sign of $n_2 - n_1$; we will assume this sign negative in the following, so that only $\phi(z) = \phi_+(z)$ will be considered. From Eq. (12) and from the monotonicity of $K(z)$, we see that for every angular frequency ω, there is a unique position $z(\omega)$ in the crystal in which energy transfer occurs between the two modes and that is given by

$$K[z(\omega)] = k_1(\omega) - k_2(\omega) = \frac{\omega}{c}[n_1(\omega) - n_2(\omega)]. \tag{13}$$

Moreover, if $z(\omega)$ is itself monotonic, then there is for every position z inside the crystal a unique angular frequency $\omega(z)$ for which energy transfer occurs significantly.

An exact solution of the coupled-wave equations (8) and (9) can be obtained only numerically, and we will present such a numerical simulation in Subsection 4.C, but much more insight can be obtained with some minor additional assumptions. Suppose all energy is in mode 1 at the entrance of the crystal [i.e., $A_1(0) = 1$ and $A_2(0) = 0$]. This repartition will be conserved almost exactly until the vicinity of $z(\omega)$ is reached and will then remain almost constant. In the vicinity of $z(\omega)$, $\kappa(z)$, and $\phi(z)$ can be considered roughly constant so that the solution of Eqs. (8) and (9) can be obtained analytically (see, e.g., Ref. 9). The main result that is then obtained is that

$$A_2(z) \approx a(\omega)\exp\{i\phi[z(\omega)]\}, \quad z > z(\omega), \tag{14}$$

where $a(\omega)$ has a modulus smaller than 1. When it leaves the crystal at position $z = L$, mode 2 has acquired the following phase:

$$\varphi(\omega) = k_2(\omega)L - \phi[z(\omega)] = k_1(\omega)z(\omega) - \psi[z(\omega)] + k_2(\omega)[L - z(\omega)]. \tag{15}$$

The three terms in this equation correspond to propagation on mode 1 for distance $z(\omega)$, interaction with the acoustic wave, and propagation on mode 2 for distance $L - z(\omega)$, respectively. The group delay encountered by every spectral component is the derivative of the above spectral phase and reads as

$$\tau(\omega) = \frac{\mathrm{d}z(\omega)}{\mathrm{d}\omega}\{k_1(\omega) - k_2(\omega) - K[z(\omega)]\} + \frac{\mathrm{d}k_1(\omega)}{\mathrm{d}\omega}z(\omega) + \frac{\mathrm{d}k_2(\omega)}{\mathrm{d}\omega}[L - z(\omega)]. \tag{16}$$

The first term is zero according to the phase-matching condition [Eq. (12)]. With the group velocity defined by $v_g(\omega) = \mathrm{d}\omega/\mathrm{d}k(\omega)$, the group delay becomes

$$\tau(\omega) = \frac{z(\omega)}{v_{g1}(\omega)} + \frac{L - z(\omega)}{v_{g2}(\omega)}. \tag{17}$$

The physical explanation of this equation is rather simple: Propagation occurs at velocity $v_{g1}(\omega)$ for distance $z(\omega)$ and subsequently at velocity $v_{g2}(\omega)$. As the interaction was assumed to be localized around $z(\omega)$, it is no surprise that the influence of this interaction has disappeared in terms of the group-delay time. We thus have proved that the phenomenological approach of Section 2 is indeed supported by coupled-wave analysis, provided that the interaction region for each frequency is small. The quality of the resulting prediction for the group delay, Eq. (17), will then depend on the ratio of this interaction length to the crystal length L.

C. Group-Delay Control

We now discuss the control of the group-delay distribution through specification of the acoustic wave characteristics. It is useful to introduce the differential group velocity between the two modes as

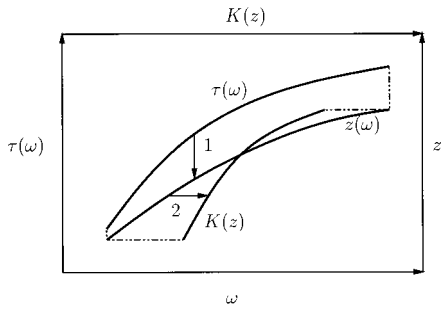

Fig. 2. Graphical representation of the computation of the acoustic signal given a desired group-delay function $\tau(\omega)$. The group-delay equation (20) gives $z(\omega)$; i.e., the position at which phase matching should occur for each frequency (arrow 1). The phase-matching condition [Eq. (21)] then gives the acoustic frequency $K(z)$ (arrow 2).

$$\Delta v_g(\omega) = [1/v_{g1}(\omega) - 1/v_{g2}(\omega)]^{-1}, \tag{18}$$

so that Eq. (17) becomes

$$\tau(\omega) = \frac{z(\omega)}{\Delta v_g(\omega)} + \frac{L}{v_{g2}(\omega)} \tag{19}$$

or, equivalently,

$$z(\omega) = \Delta v_g(\omega)\left[\tau(\omega) - \frac{L}{v_{g2}(\omega)}\right]. \tag{20}$$

Note that although we have chosen to express the previous equations by use of group velocities, we could equally well have used group indices defined by $n_g(\omega) = (\mathrm{d}/\mathrm{d}\omega) \times [n(\omega)\omega]$ and $\Delta n_g(\omega) = n_{g1}(\omega) - n_{g2}(\omega)$, since then $v_g(\omega) = c/n_g(\omega)$ and $\Delta v_g(\omega) = c/\Delta n_g(\omega)$. Given a desired group-delay distribution, Eq. (20) dictates the position of phase matching for every frequency. Note that if the crystal were not dispersive, this relation would be linear. The phase-matching condition [Eq. (13)] then specifies the form of the acoustic signal and can be rewritten as

$$K[z(\omega)] = \frac{\omega}{\Delta v_p(\omega)}, \tag{21}$$

where $\Delta v_p(\omega) = c/[n_2(\omega) - n_1(\omega)]$ is the differential phase velocity between the two modes. Eqs. (20) and (21) determine completely the form of the acoustic wave when an arbitrary group delay is specified. This process is summarized in Fig. 2. The first step is to specify $\tau(\omega)$ as a function of ω, then to compute $z(\omega)$ from Eq. (20), and finally to obtain $K[z(\omega)]$ from Eq. (21). Hence a parametric representation of $K(z)$ as a function of z is obtained.

In the important case of a linear chirp, or

$$\tau(\omega) = D\omega + \tau_0, \tag{22}$$

where D is group-delay dispersion (GDD) in squared femtoseconds and τ_0 some constant delay time, insertion of Eqs. (19) and (22) into Eq. (21) gives

$$K[z(\omega)] = \frac{1}{D\Delta v_p(\omega)}\left[\frac{z(\omega)}{\Delta v_g(\omega)} + \frac{L}{v_{g2}(\omega)} - \tau_0\right]. \tag{23}$$

If the different velocities involved would have constant values, which is the case for small bandwidths, then the acoustic signal would also be linearly chirped, with a slope given by $(\Delta v_p \Delta v_g D)^{-1}$.

D. Self-Compensation

In some applications, before trying to introduce a given group-delay distribution, the material dispersion of the crystal itself should first be compensated for. When self-compensation is obtained, the group delay should be a constant value T for every frequency ω, and Eq. (20) gives

$$z(\omega) = \Delta v_g(\omega)\left[T - \frac{L}{v_{g2}(\omega)}\right]. \tag{24}$$

It is then clear that the bandwidth that can be accommodated for is limited by the condition that some delay T can be found such that $0 \leqslant z(\omega) \leqslant L$ for every frequency ω in that bandwidth. Expliciting this condition with the assumption $\Delta v_g(\omega) > 0$ simply gives that for every frequency

$$\frac{L}{v_{g2}(\omega)} \leqslant T \leqslant \frac{L}{v_{g1}(\omega)}, \tag{25}$$

which is equivalent to the following condition:

$$\max_{\omega}[v_{g1}(\omega)] \leqslant \min_{\omega}[v_{g2}(\omega)]. \tag{26}$$

This inequality would be reversed if $\Delta v_g(\omega) < 0$. Equation (26) defines the bandwidth in which the acoustic interaction is able to compensate for the dispersion of its host crystal. It means that the group velocity of the fastest frequency for mode 1 should be less than the group velocity of the slowest frequency for mode 2. This condition is illustrated by Fig. 3. For every frequency ω, the effective group velocity on propagation through the crystal is given by

$$v_g(\omega) = \left[\frac{z(\omega)}{L}\frac{1}{v_{g1}(\omega)} + \frac{L - z(\omega)}{L}\frac{1}{v_{g2}(\omega)}\right]^{-1}. \tag{27}$$

It is obviously a weighted average of the group velocities for both modes. As depicted in Fig. 3, for every frequency, the effective group velocity has a range of possible values extending from $v_{g1}(\omega)$ to $v_{g2}(\omega)$. If all frequencies have to share a common effective group velocity V, i.e., a common group delay $T = L/V$, then V has to be in the range of all frequencies, hence condition (26). This representation can be immediately generalized for an arbitrary group-delay function $\tau(\omega)$, just by defining the effective group velocity $v_g(\omega) = L/\tau(\omega)$ that must satisfy

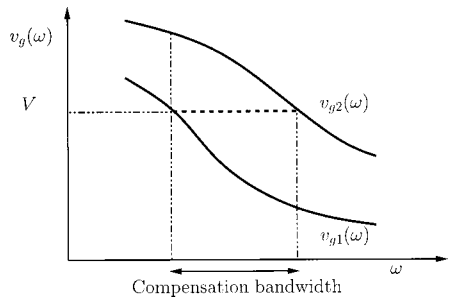

Fig. 3. Determination of the compensation bandwidth. $v_{g1}(\omega)$ and $v_{g2}(\omega)$ are the optical group velocities on modes 1 and 2, respectively; $v_g(\omega)$ is the group delay of the diffracted pulse.

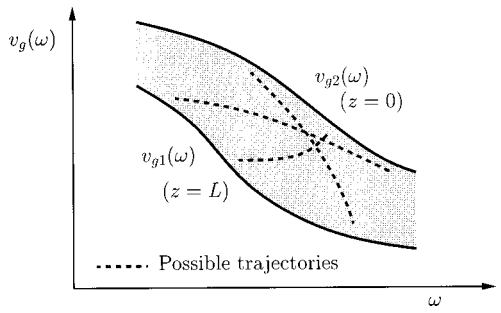

Fig. 4. Possible group-delay trajectories. The AOPDF can impose an arbitrary group-delay variation $\tau(\omega)$ on the diffracted optical pulse, provided that the corresponding group velocity $v_g(\omega) = L/\tau(\omega)$ remains between $v_{g1}(\omega)$ and $v_{g2}(\omega)$.

Eq. (27). As depicted in Fig. 4, the required trajectory $v_g(\omega)$ must lie within the region delimited by curves $v_{g1}(\omega)$ and $v_{g2}(\omega)$.

4. ACOUSTO-OPTIC INTERACTION

A. Collinear Interaction

The volume gratings that have been considered in Section 3 were assumed static. However, the acoustic waves usually used are progressive with a given velocity V and are generated by applying a rf signal to a transducer bonded to the crystal. Like optical waves, the acoustic wave is dispersive; i.e., a phase velocity and a group velocity can be defined. Anyway, it is the phase velocity we are concerned with through phase matching. For the sake of simplicity, we will consider this velocity constant in the following. The rf signal must have the form

$$s(t) = \cos\left[\int_0^t \Omega(t)\mathrm{d}t\right], \tag{28}$$

with the instantaneous frequency $\Omega(t)$ given by

$$\Omega(t) = VK(Vt). \tag{29}$$

Hence the temporal signal to be applied to the transducer can be computed easily from $K(z)$. For instance, in the case of the linear chirp of Eq. (22), the corresponding temporal chirp would be

$$\Omega(t) = \frac{V}{\Delta v_p}\frac{V}{\Delta v_g}\frac{t}{D} + \Omega_0, \tag{30}$$

where Ω_0 is some constant frequency.

Another consequence of the progressive nature of the acoustic wave is that a sequence of short pulses will see the fixed acoustic grating that is the same but that starts at a different location z_0 ($z_0 = 0$ was assumed in the preceding analysis). For each frequency, propagation will occur for distance $z_0 + z(\omega)$ on mode 1 and then for distance $L - z_0 - z(\omega)$ on mode 2. The group delay will then be

$$\tau_{z_0}(\omega) = \tau(\omega) + \frac{z_0}{\Delta v_g(\omega)}, \tag{31}$$

where $\tau(\omega)$ is the group delay of Eq. (19). The second term in Eq. (31) is a variable jitter. For most applications, the existence of this jitter will not be a problem, provided that it remains nondispersive, a condition that can hold only for small bandwidths in general. If it is dispersive, then this effect can be corrected by synchronization of the acoustic wave generation with the pulsed laser source.

B. Quasi-Collinear Interaction

In the preceding analysis, we have considered implicitly that the optical and acoustic waves were collinear in both the phase and the group-velocity sense. However, in the vast majority of efficient acousto-optic interactions, this assumption is not verified, and all six directions defined by the phase and the group velocities of the two optical waves and of the acoustic wave can be different. Anyway, this situation has been treated extensively; see, e.g., Ref. 9, at least for the case of the diffraction of a monochromatic optical wave on a fixed-frequency acoustic wave. We will restrict our attention to the quasi-collinear case depicted in Fig. 5. We still assume that the phase velocity of the acoustic wave is directed along the z axis, but the wave vectors of the two optical modes now have an x component and Eq. (4) becomes

$$\begin{aligned}\mathbf{E}_m(\omega, \mathbf{r}) &= \sqrt{S(\omega)}\mathbf{e}_m \exp[-i\mathbf{k}_m(\omega)\cdot\mathbf{r}] \\ &= \sqrt{S(\omega)}\mathbf{e}_m \exp\{-i[\alpha_m(\omega)x + \beta_m(\omega)z]\},\end{aligned} \tag{32}$$

with the normalization of Eq. (5) unchanged. The phase and group velocities are different for axes x and z and read, respectively, $v_{pmx} = \omega/\alpha_m(\omega)$ and $v_{pm} = \omega/\beta_m(\omega)$, and $v_{gmx} = \mathrm{d}\omega/\mathrm{d}\alpha_m(\omega)$ and $v_{gmz} = \mathrm{d}\omega/\mathrm{d}\beta_m(\omega)$. The wave equation (6) is unchanged, and the mode envelopes A_1 and A_2 depend only on z as before. Replacement of Eq. (4) by Eq. (32) then leads to the same coupled-wave equations as in Subsection 3.B but with

$$\phi(z) = [\beta_2(\omega) - \beta_1(\omega)]z - \psi(z) \tag{33}$$

and the phase-matching conditions

$$\alpha_2(\omega) = \alpha_1(\omega), \tag{34}$$

$$K(z) = \beta_2(\omega) - \beta_1(\omega). \tag{35}$$

The first condition implies that the phase velocity and the group velocity are identical for both modes along the x axis, and the last condition still defines $z(\omega)$. The phase of Eq. (15) at any point $\mathbf{r}$ after the interaction has occurred becomes

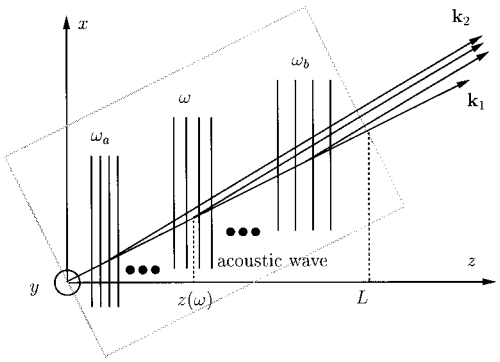

Fig. 5. Representation of the quasi-collinear acousto-optic interaction geometry.

$$\varphi(\omega) = \mathbf{k}_2(\omega) \cdot \mathbf{r} - \phi[z(\omega)]. \tag{36}$$

The derivative of this phase is the group delay and reads with $\mathbf{r} = (x, L)$:

$$\tau(\omega) = \frac{z(\omega)}{v_{g1z}(\omega)} + \frac{L - z(\omega)}{v_{g2z}(\omega)} + \frac{x}{v_{gx}(\omega)}. \tag{37}$$

Note that the interaction length L is measured along the z axis, and x is the abscissa of the output beam at the end of the crystal. Expression (37) for the group delay in the quasi-collinear case is identical to expression (17) for the group delay in the collinear case, except for the spatial chirp term $x/v_{gx}(\omega)$. This group-delay term is directly connected to the geometrical walk-off between the incident beam and the diffracted beam and has no influence on the group-delay control. If the spatial chirp is to remain small, and when the finite size of the beams is taken into account, the collinearity or quasi-collinearity of the group velocities of the two optical modes should be stressed. However, for the AOPDF operating in a quasi-collinear configuration described in Ref. 10, the spatial chirped was not observed.

C. Numerical Simulations

To illustrate the previous mathematical development, we have performed numerical simulations for the interaction geometry in a $L = 3$-cm-long TeO_2 crystal in a quasi-collinear configuration.[10] This geometry is intended for group-delay control of titanium:sapphire ultrashort laser pulses, i.e., with a central wavelength of 800 nm, and has been designed so that the interaction is efficient. The two modes used are polarized along the ordinary and extraordinary axes; at $\lambda = 800$ nm, $n_0 = 2.226$, and $n_e = 2.374$. Dispersion data for TeO_2 are taken from Ref. 11, page 33.66. The application of the criterion [Eq. (26)] indicates that dispersion compensation can be obtained at least from 700 to 900 nm; the corresponding rf frequency range extends from 40 to 60 MHz. In this case the acoustic signal occupies ~58% of the crystal length. Figure 6 shows the spectral intensity and phase that are induced on mode 2 when the acoustic signal is computed from Eq. (24). The constant group delay T equals ~240 ps. Propagation is simulated frequency by frequency by numerical integration of the coupled-wave equations, i.e., without the further approximations used to derive an analytical formula for the group delay. The coupling constant is chosen so that $\kappa L = 30$; i.e., this is a rather strong coupling. The spectral intensity has a shape characteristic of the Gibbs phenomenon, well known in Fourier analysis[12]: The amplitude of the acoustic signal is constant between 700 and 900 nm, and zero elsewhere; high spatial frequencies are not resolved by the diffracted optical beam and result in rapid oscillations of the spectral intensity. Anyway, these could be reduced by an adequate apodization. The target phase ωT has been removed from the computed phase to show that the desired goal has been achieved: Only slight high-frequency phase fluctuations remain around the mean value. The parabolic variation of the phase outside the target bandwidth is characteristic of the material dispersion. The group delay computed by numerical differentiation from the spectral phase of Fig. 6 is shown in Fig. 7. The oscillations of the spectral phase are seen to be amplified by the differentiation but still have the same high-frequency character with a zero mean. Experimentally, such oscillations in the spectral phase or in the group delay cannot be resolved during measurement, and a mean value would be obtained instead. Furthermore, the effect on the temporal shape of the diffracted pulse of the oscillatory behavior of the spectral phase is integrated [see Eq. (3)]. This should result in the temporal domain in a modulation of the pulse some distance away from the correctly compressed central part of the pulse. To verify this assumption, we simulated the propagation of a 15-fs Gaussian pulse through the crystal. Figure 8 shows the incident 15-fs pulse and the 3.3-ps dispersed pulse at the output of the crystal on mode 1 if no acoustic signal were applied. When the acoustic signal is computed from Eq. (24), a 15.3-fs pulse is retrieved on mode 2, as shown also

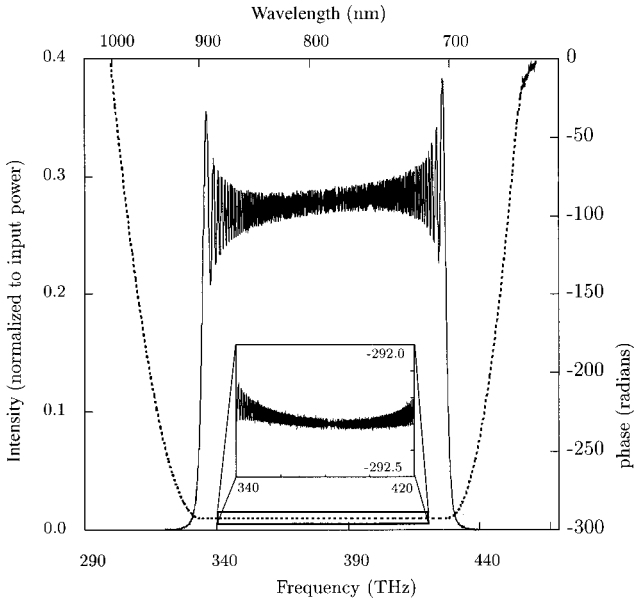

Fig. 6. Spectral intensity and phase induced on mode 2 when the acoustic signal is computed from Eq. (24) for a 3-cm-long collinear AOPDF. The inset shows a magnified portion of the spectral phase versus frequency curve.

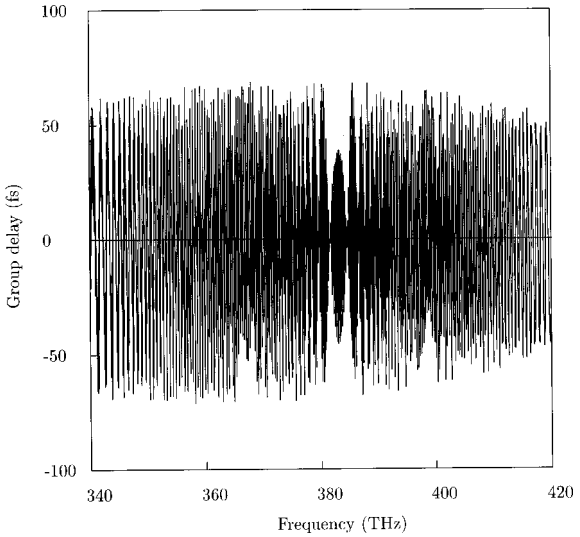

Fig. 7. Group delay computed from the spectral phase of Fig. 6.

in Fig. 8. It can be seen that the rapid oscillations in the spectral intensity and phase caused by the acousto-optic interaction yield only small pulse pedestals, as predicted.

As said above, the acoustic signal needed to compensate for the dispersion of the TeO_2 crystal occupies ~58% of the crystal length for the 700- to 900-nm bandwidth, and this corresponds to a total group delay of ~9.2 ps. The remaining 42% of the crystal length can induce a further total of 6.7 ps of programmable negative dispersion. Figure 9 shows five examples of such group-delay control. The desired dispersion is specified by the values of the GDD, in squared femtoseconds, and of the third-order dispersion, in cubed femtoseconds, as listed in Table 1. Example number 3 yields the largest total group delay and corresponds to an acoustic signal that occupies ~95% of the crystal length. Also listed in Table 1 are the values of the GDD and the third-order dispersion obtained when the group-delay curves obtained are fitted with a polynomial model of the second degree. It can be seen that the obtained dispersion values are not exactly those that were designed, although they remain relatively close, and that this mismatch increases with the desired dispersion. Note that the effect seems absent when a constant group delay is required, as shown in Fig. 7. We believe that the mismatch between the predicted value of the group delay and the simulated value comes from the stationary phase approximation used, i.e., in Eq. (14), but we are unable presently to provide a sound argument to support this hypothesis and leave this discussion open. Anyway, from a practical point of view, if one is to obtain a specific group-delay variation specified, e.g., by its GDD and third-order dispersion, a computer optimization can be performed to obtain the required acoustic signal. However, the practical usefulness of such an approach will depend on the computation time. For the examples presented in Fig. 9, 8196 sampling points are used for the z axis, while 4096 sampling points are used for the optical angular frequency axis. These rather large numbers are dictated by the necessity of resolving the acoustic fringes and the rapid fluctuations of the group delay, respectively. The overall computation time per curve is ~15 min on an Ultra 1 Sun workstation. Reduction of this computation time is needed for implementing an optimization procedure; this could probably be achieved by improving the numerical simulation method used.

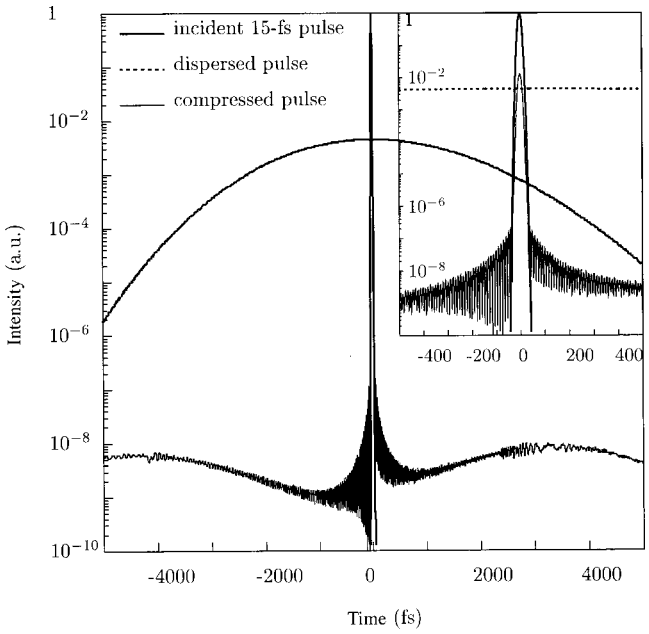

Fig. 8. Numerical simulation of the propagation of an incident 15-fs Gaussian pulse through a 3-cm-long collinear AOPDF. The spectrum of the incident pulse is centered on 380 THz and is 29.4-THz FWHM large. The inset shows the magnified central portion of the curves.

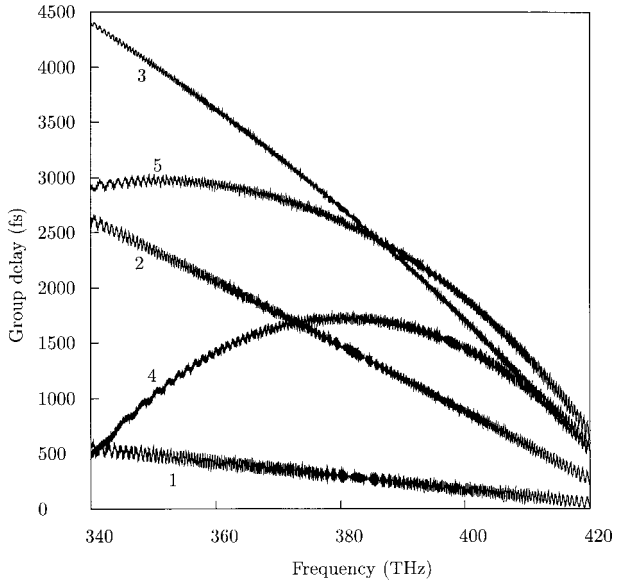

Fig. 9. Five examples of group-delay control. Table 1 lists the designed versus the obtained dispersion values.

Table 1. Designed Versus Obtained Dispersion Values for the Five Examples of Fig. 9

Curve	Designed		Obtained	
	GDD (fs^2)	TOD (fs^3)	GDD (fs^2)	TOD (fs^3)
1	−1000	0	−996	34
2	−5000	0	−4690	−1185
3	−10000	0	−7652	−8610
4	0	−40000	196	−37850
5	−5000	−30000	−4244	−24955

5. CONCLUSION

We have studied the operation of AOPDF's in either bulk or integrated configurations. We have obtained a simple analytical expression for the group delay imposed on a diffracted optical short pulse by a general chirped acoustic wave. Furthermore, we have shown that an arbitrary, although monotonic, group delay can be obtained by proper specification of the acoustic signal. This transposition of the control of the spectral phase of an optical pulse to the control of a rf temporal signal has the strong practical advantage of direct computer control with an arbitrary accuracy. Computer simulations were performed to verify the theoretical predictions and were shown to support them except for a slight mismatch for large dispersions.

ACKNOWLEDGMENTS

The authors acknowledge fruitful discussions with D. Dolfi and L. Morvan of Thomson-CSF, Corporate Research Laboratory, and J. Desbois of Thomson-CSF, Microsonics.

REFERENCES

1. A. M. Weiner, D. E. Leaird, J. S. Patel, and J. R. Wullert II, "Programmable shaping of femtosecond optical pulses by use of 128-element liquid-crystal phase modulator," IEEE J. Quantum Electron. **28**, 908–919 (1992).
2. M. A. Wefers and K. A. Nelson, "Programmable phase and amplitude femtosecond pulse shaping," Opt. Lett. **18**, 2032–2034 (1993).
3. M. A. Wefers and K. A. Nelson, "Analysis of programmable ultrashort waveform generation using liquid-crystal spatial light modulators," J. Opt. Soc. Am. B **12**, 1343–1362 (1995).
4. K. M. Mahoney and A. M. Weiner, "A femtosecond pulse-shaping apparatus containing microlens arrays for use with pixellated spatial light modulators," IEEE J. Quantum Electron. **32**, 2071–2077 (1996).
5. C. Dorrer, F. Salin, F. Verluise, and J.-P. Huignard, "Programmable phase control of femtosecond pulses by use of a nonpixelated spatial light modulator," Opt. Lett. **23**, 709–711 (1998).
6. A. Efimov, M. D. Moores, N. M. Beach, J. L. Krause, and D. H. Reitze, "Adaptive control of pulse phase in a chirped-pulse amplifier," Opt. Lett. **23**, 1915–1917 (1998).
7. M. E. Fermann, V. da Silva, D. A. Smith, Y. Silberberg, and A. M. Weiner, "Shaping of ultrashort optical pulses by using an integrated acousto-optic tunable filter," Opt. Lett. **18**, 1505–1507 (1993).
8. P. Tournois, "Acousto-optic programmable dispersive filter for adaptive compensation of group delay time dispersion in laser systems," Opt. Commun. **140**, 245–249 (1997).
9. A. Yariv and P. Yeh, *Optical Waves in Crystals* (Wiley, New York, 1984).
10. F. Verluise, V. Laude, J.-P. Huignard, and P. Tournois, "Design of an improved acousto-optic programmable dispersive filter," in *Conference on Lasers and Electro-Optics (CLEO/U.S.)*, Vol. 6 of 1998 OSA Technical Digest Series (Optical Society of America, Washington D.C., 1998), p. 99.
11. M. Bass, ed., *Handbook of Optics*, 2nd ed. (McGraw-Hill, New York, 1995).
12. D. F. Elliot, ed., *Handbook of Digital Signal Processing* (Academic, San Diego, 1986).